



Rotational giant magnetoimpedance in soft magnetic wires: Modelization through Fourier harmonic contribution

C. Gómez-Polo, M. Vázquez, and M. Knobel

Citation: [Applied Physics Letters](#) **78**, 246 (2001); doi: 10.1063/1.1336814

View online: <http://dx.doi.org/10.1063/1.1336814>

View Table of Contents: <http://scitation.aip.org/content/aip/journal/apl/78/2?ver=pdfcov>

Published by the [AIP Publishing](#)

Articles you may be interested in

[Valve behavior of giant magnetoimpedance in field-annealed Co 70 Fe 5 Si 15 Nb 2.2 Cu 0.8 B 7 amorphous ribbon](#)

J. Appl. Phys. **97**, 10M108 (2005); 10.1063/1.1854891

[Giant magnetoimpedance of amorphous ribbon/Cu/amorphous ribbon trilayer microstructures](#)

J. Appl. Phys. **95**, 1364 (2004); 10.1063/1.1634389

[Giant magnetoimpedance in trilayer structures of patterned magnetic amorphous ribbons](#)

Appl. Phys. Lett. **81**, 1654 (2002); 10.1063/1.1499769

[Permeability and giant magnetoimpedance in Co 69 Fe 4.5 X 1.5 Si 10 B 15 \(X=Cr , Mn, Ni\) amorphous ribbons](#)

J. Appl. Phys. **89**, 7218 (2001); 10.1063/1.1359226

[Anisotropy and magnetization processes in Co-rich amorphous wires](#)

J. Appl. Phys. **85**, 5441 (1999); 10.1063/1.369969



AIP | Journal of
Applied Physics

Journal of Applied Physics is pleased to
announce **André Anders** as its new Editor-in-Chief

Rotational giant magnetoimpedance in soft magnetic wires: Modelization through Fourier harmonic contribution

C. Gómez-Polo^{a)}

Departamento de Física, Universidad Pública de Navarra, Campus de Arrosadia, 31006 Pamplona, Spain

M. Vázquez

Instituto Ciencia de Materiales and Instituto Magnetismo Aplicado, CSIC, Campus de Cantoblanco, 28049 Madrid, Spain

M. Knobel

Instituto de Física "Gleb Wataghin," Universidade Estadual de Campinas (UNICAMP), C. P. 6165, 13.083-970 Campinas, São Paulo, Brazil

(Received 13 June 2000; accepted for publication 3 November 2000)

A method to investigate the giant magnetoimpedance effect based on Fourier analysis is introduced. The study is carried out on a FeCoSiB amorphous wire with vanishing magnetostriction subjected to joule heating (current annealing) treatment that induces an enhancement of circumferential magnetic anisotropy and modifies the magnetoimpedance response of the samples. Experimental results are interpreted within the framework of the classical electrodynamic model, where the circumferential permeability plays the dominant role in the field dependence of the complex impedance of the sample. A rotational magnetization model is employed to determine the circular magnetization process, and a mean value of the circumferential permeability is obtained through the harmonic components obtained through Fourier analysis of the time derivative of the circular magnetization. This simple model is able to reproduce the observed experimental behavior, i.e., evolution of the field dependence of the complex impedance with annealing and the asymmetrical field dependence under a dc biased electrical current. © 2001 American Institute of Physics.

[DOI: 10.1063/1.1336814]

The magnetotransport properties of nanostructured materials have been extensively studied during the last few decades.¹ Among them the so-called giant magnetoimpedance (GMI) effect stands out, in which the high frequency impedance of a high-permeability material sensitively changes upon the application of an external dc magnetic field.² Its main interest lies in the technological field, since new sensitive and quick response micromagnetic sensors can be developed based on amorphous³ and nanocrystalline⁴ wires, ribbons,⁵ and thin films.⁶

The origin of the effect can be rather well understood within the framework of classical electrodynamics.⁷ Let us consider the case of metallic magnetic wires. When an ac current, $I = I_0 e^{-i2\pi ft}$, flows through the wire for high enough current frequency, f , it mainly concentrates in a reduced region (outer shell) close to the sample surface (skin-effect). Under these circumstances, the complex impedance Z , can be expressed as a function of the Bessel functions of the first kind, J_i :

$$Z = \frac{1}{2} R_{dc} k a \frac{J_0(ka)}{J_1(ka)} \quad (1)$$

with $k = \sqrt{i2\pi\mu_\phi f/\rho}$, μ_ϕ : circumferential permeability, ρ : electrical resistivity, a : wire radius, $R_{dc} = (\rho L/\pi a^2)$ where L : sample length. Thus, in a ferromagnetic sample the circular magnetization process mainly dominates the GMI response through the evolution of μ_ϕ under the external dc field, H . When the wire is magnetically soft, i.e., when the

permeability is strongly influenced by a relatively small magnetic field, one observes a huge variation of the material's impedance, giving rise to the GMI effect.

Different approaches have been employed to estimate $\mu_\phi(H)$. First, at high exciting frequencies (megahertz range), where the domain wall contribution can be neglected, the ferromagnetic resonance treatment is applicable in the analysis of the GMI.^{8,9} For lower driving frequencies (kilohertz range) where the skin effect still dominates the impedance behavior, two different approaches have been employed: the estimation of μ_ϕ associated to domain wall movements^{10,11} and the analysis of the circular magnetization process, that is, $\mu_\phi(H)$, through the minimization of the energy equation associated to the magnetization rotation.^{12,13} This last approach satisfactorily explains the GMI behavior in those cases where the magnetization rotation contribution dominates the circular magnetization process, i.e., reinforcement of the circumferential anisotropy through convenient thermal treatments.¹⁴

However, the classical electrodynamic model [Eq. (1)] is based on the assumption of a constant value of μ_ϕ during the circular magnetization process. It is quite clear that just in few particular cases this last assumption is strictly valid. In order to overcome this restriction, the approximation of small circular magnetic field,¹⁵ H_ϕ is taken irrespectively of the actual circular magnetization process. Although this approximation can be considered valid for low enough amplitude current values, I_0 , is not extensively valid for any real GMI case.

In this sense, the aim of this letter is to present the Fourier analysis as a powerful tool to estimate $\mu_\phi(H)$, and thus,

^{a)}Electronic mail: gpolo@unavarra.es

the GMI effect. In particular, in amorphous FeCoSiB joule heated wires the Fourier analysis of the time derivative of the calculated circular magnetization allows us to determine $\mu_\phi(H)$ and thus to reproduce the experimental field dependence of the electrical impedance of the wires.

The amorphous wires with nominal composition $(\text{Fe}_{0.06}\text{Co}_{0.94})_{72.5}\text{Si}_{12.5}\text{B}_{15}$ were obtained by the so-called ‘‘in-rotating-water quenching technique’’ with mean diameter of 120 μm . Pieces 8 cm in length were submitted to subsequent current annealings at current densities, $j=19.9$ and 24.3 A/mm^2 during 5 min. Since the Curie point corresponds to a current density of 32.1 A/mm^2 , the induction of a circumferential anisotropy K_ϕ takes place under the performed thermal treatment.¹⁶ With respect to the GMI measurements, the voltage drop across the wire and in a resistor (connected in series to monitor the sinusoidal ac current) were simultaneously recorded through a digital oscilloscope. The real and imaginary components of the impedance were registered through a dual phase lock-in amplifier. Longitudinal dc magnetic fields were created by a long solenoid (36.6 Oe/A) and axial hysteresis loops were also obtained using an ac conventional induction method.

Within the framework of a rotational magnetization process, the equilibrium angle, θ , of the magnetization M_s with respect to the circumferential direction, ϕ , can be calculated by minimizing the energy equation

$$E = K_\phi \sin^2(\theta - \theta_K) - \mu_0 M_s H \sin \theta - \mu_0 M_s H_\phi \cos \theta, \quad (2)$$

where θ_K is a skew angle of the easy magnetization direction with respect to ϕ . Thus, the magnetization $M_\phi(t) = M_s \cos[\theta(t)]$ response to the field $H_\phi = H_0 \cos(2\pi ft)$ can be calculated, $M_\phi(t)$ numerically derived and its Fourier components calculated

$$a = \frac{2}{T} \int_0^T \frac{\partial M_\phi(t)}{\partial t} \cos(2\pi ft) dt; \quad (3)$$

$$b = \frac{2}{T} \int_0^T \frac{\partial M_\phi(t)}{\partial t} \sin(2\pi ft) dt.$$

The earlier Fourier coefficients allow the determination of the circumferential permeability: $\mu_\phi = \mu_0 C(-b + ia)$, with C a constant equal to $C = 1/2\pi f H_0$.

Figure 1 shows the axial field evolution of the resistive (R) and reactive component (X) of the complex impedance, $Z = R + iX$, for the as-cast and Joule heated wires ($f = 50$ kHz, $I_{ac}(\text{rms}) = 5$ mA). The line figures correspond with the calculated $R(H)$ and an $X(H)$ evolution with the following data: $\rho = 135 \mu\Omega \text{ cm}$; $a = 60 \mu\text{m}$; $L = 6$ cm (mean distance between voltage contacts); $H_0 = 0.24$ Oe. Table I summarizes the fitting parameters for the as-cast and annealed wires. The K_ϕ values are directly obtained from the anisotropy field, $H_K = 2K_\phi/\mu_0 M_s$, estimated through the axial hysteresis loops. Both C and θ_K parameters are obtained minimizing the difference between the experimental and the estimated impedance values. Notice the closeness between the fitting and theoretical expected C values [$C = 1/2\pi f H_0 = 1.7 \cdot 10^{-7} \text{ s(A/m)}^{-1}$]. As an example, the inset of Fig. 1 shows the calculated circular hysteresis loop ($M_\phi - H_\phi$) for $K_\phi = 19.9 \text{ J/m}^3$ ($j = 24.3 \text{ A/mm}^2$) and $H = 0.3$ Oe (H_ϕ in Oe).

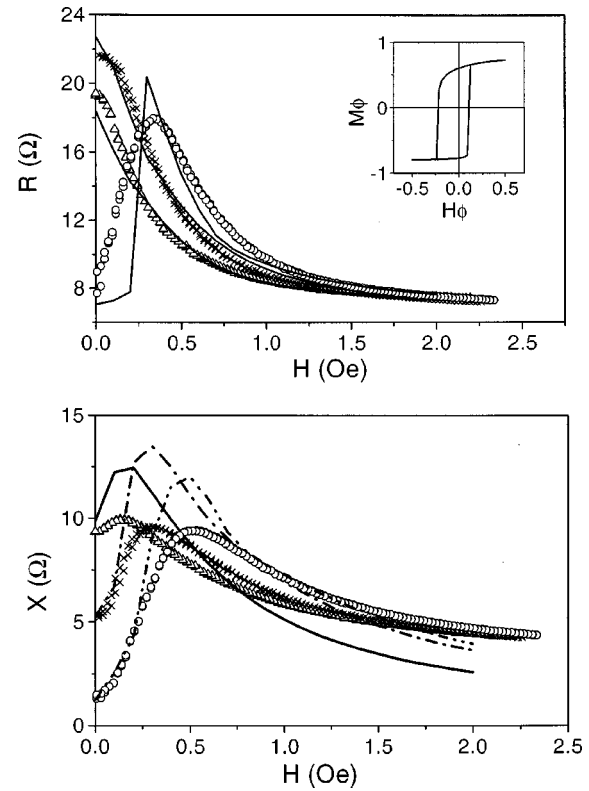


FIG. 1. Comparison between the calculated (line) and experimental (symbols) axial field (H) dependence of impedance components, $Z = R + iX$, ($f = 50$ kHz, $I_{ac} = 5$ mA) for (Δ) as-cast and joule heated wires at $j = 19.9$ (\times) and 24.3 (\circ) A/mm^2 . The inset shows the estimated circular $M_\phi - H_\phi$ hysteresis loops for $K_\phi = 19.9 \text{ J/m}^3$ ($j = 24.3 \text{ A/mm}^2$) and $H = 0.3$ Oe.

It is important to remark that the permeability behavior seems to be mainly dominated by the circular magnetization process of the region close to the wire surface, since the best fitting curves are obtained considering $H_0 = I_0/2\pi a \approx 0.24$ Oe. In fact, a similar, but more complex estimation was performed considering the radial dependence of the circular magnetic field, $H_0 = (I_0/2\pi a)(r/a)$, subdividing the total sample volume along the radial coordinate in regions where H_ϕ was considered constant and calculating the contribution of each region to the total circular magnetization process. Surprisingly, the obtained fitting curves do not reproduce so fairly well the experimental results. Whether this rough approximation ($H_\phi \approx I_0/2\pi a$) has or not some physical meaning (i.e., interplay of the exchange forces during the circular magnetization process so that the external region $r \approx a$ plays the dominant role) must be analyzed in further detail.

On the other hand, to obtain the best fitting curves it is necessary to consider the existence of a skew angle θ_K

TABLE I. Fitting parameters for the as-cast and joule heated wires (heating current density, j): circumferential anisotropy, K_ϕ , associated anisotropy field, H_k , and C constant.

$j(\text{A}/\text{mm}^2)$	$K_\phi(\text{J}/\text{m}^3)$	$H_k(\text{Oe})$	θ_K	$C[\text{s(A/m)}^{-1}]$
As-cast	6.4	0.2	$\pi/10$	1.1×10^{-7}
19.9	11.9	0.4	$\pi/10$	1.5×10^{-7}
24.3	19.9	0.6	$\pi/10$	1.6×10^{-7}
24.3 ^a	19.9	0.6	$\pi/10$	1.4×10^{-7}

^aBiased current.

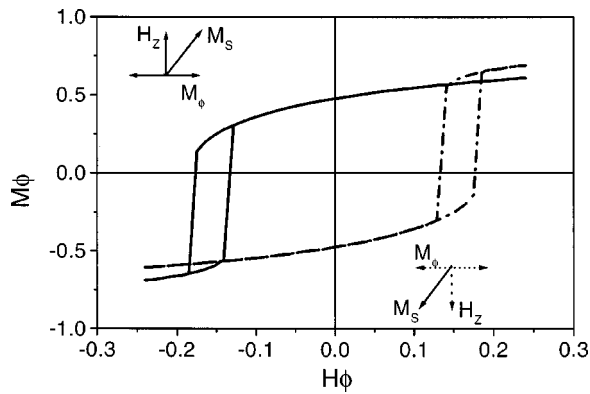


FIG. 2. Calculated circular hysteresis loops, $M_\phi-H_\phi$, ($K_\phi=19.9\text{ J/m}^3$) for $H=0.5\text{ Oe}$ (solid line) and $H=-0.5\text{ Oe}$ (dot line).

$=\pi/10$, whose main consequence is the occurrence of an asymmetrical behavior in the circular $M_\phi-H_\phi$ magnetization process for both θ_K and H not null [see inset of Fig. 1].

Thus, we can conclude that with this simple method it is possible to reproduce fairly well the field dependence of the complex impedance. A natural extension of the present approach is to consider a distribution of anisotropy axes and the domain wall contribution, which will certainly improve the fitting of experimental data (i.e., existence of hysteresis in the GMI field evolution). However, the present oversimplified method is already enough to reproduce the main characteristics of the impedance behavior.

With respect to the GMI evolution for $H<0$, Fig. 2 shows as an example the calculated $M_\phi-H_\phi$ hysteresis loops for the annealed wire at $j=24.3\text{ A/mm}^2$, with $H=0.5$ (solid line) and $H=-0.5$ (dot line). The observed symmetrical behavior with respect to H , gives rise to a symmetrical evolution of $\mu_\phi(H)$, and would explain the observed symmetrical experimental $Z(H)$ curves. However, it is well known that an asymmetrical behavior can be experimentally found when applying a dc bias field (i.e., twisted wire under a dc biased current) that is of great importance regarding sensor design (increase of the linear field response of the device).¹⁷

In order to analyze if this simple model could also explain the asymmetrical GMI behavior, the field dependence of Z was measured for the annealed wire at $j=24.3\text{ A/mm}^2$ with a dc biased current $I_{dc}=2.5\text{ mA}$ [$f=50\text{ kHz}$, $I_0(\text{rms})=5\text{ mA}$]. Figure 3 shows the comparison between the experimental and the calculated $R(H)$ and $X(H)$ taking similar fitting parameters [$\theta_K=\pi/10$, $K_\phi=19.9\text{ J/m}^3$, $C=1.410^{-7}\text{ s (A/m)}^{-1}$; see table I] and a dc biased circular field $H_{\phi,dc}=-0.057$, corresponding to the mean dc field across the wire [$\langle H_{\phi,dc} \rangle=(2/3)(I_{dc}/2\pi a)$]. From this figure, the validity of this model for this asymmetrical behavior is also demonstrated. Coming back to Fig. 2, it can be seen how a negative (counter clockwise with respect to the positive H_ϕ direction) dc biased $H_{\phi,dc}$ breaks the symmetrical behavior with respect to H . In fact, the application of a negative dc biased circular field ($H_{\phi,dc}<0$) can avoid the irreversible change in M_ϕ for $H<0$, causing a decrease in the mean value of μ_ϕ with respect to the opposite axial field direction ($H>0$). We also believe that the application of the present first harmonic analysis could help to elucidate a recent controversy regarding the asymmetrical magnetoimpedance curves in amorphous ribbons.

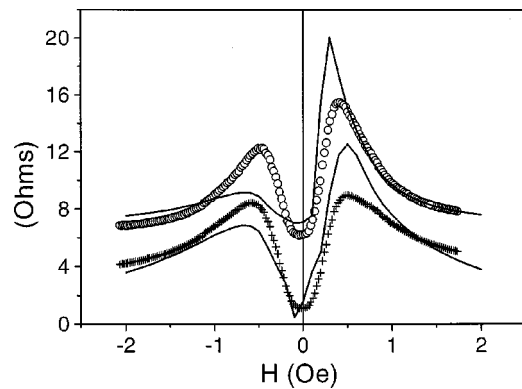


FIG. 3. Comparison between the calculated (solid line) and experimental (symbols) axial field (H) dependence of impedance components, $Z=R+iX$, ($f=50\text{ kHz}$, $I_{ac}=5\text{ mA}$) for the joule heated wire at $j=24.3\text{ A/mm}^2$ with a dc biased current $I_{dc}=2.5\text{ mA}$ [R : (\circ); X : ($+$)].

In conclusion, the field dependence of the complex impedance in as-cast and joule heated amorphous FeCoSiB wires have been presented and analyzed through a Fourier analysis of the time derivative of the calculated circular magnetization. The results show that within a simple rotational model, the experimental GMI behavior can be suitably fitted using first harmonic components of the signal to estimate the mean value of the circumferential permeability. Further developments of the model, which include the analysis of higher harmonic components, are presently under development.

This work was supported by the Spanish CICYT under Project MAT-1999-0422-C02. Brazilian agencies FAPESP and CNPq are also acknowledged.

- ¹G. Xiao, J. Q. Wang, and P. Xiong, *Appl. Phys. Lett.* **62**, 420 (1993).
- ²K. Mohri, T. Uchiyama, and L. V. Panina, *Sens. Actuators A* **59**, 1 (1997).
- ³K. V. Rao, F. B. Humphrey, and J. L. Costa-Kramer, *J. Appl. Phys.* **76**, 6204 (1994).
- ⁴M. Knobel, M. L. Sánchez, P. Marín, C. Gómez-Polo, M. Vázquez, and A. Hernando, *IEEE Trans. Magn.* **31**, 4009 (1995).
- ⁵R. L. Sommer and C. L. Chien, *Phys. Rev. B* **53**, R5982 (1996).
- ⁶T. Morikawa, Y. Nishibe, H. Yamdura, Y. Nonomura, M. Takeuchi, and T. Taga, *J. Magn. Soc. Jpn.* **20**, 553 (1996).
- ⁷L. D. Landau, E. M. Lifschitz, and L. P. Pitaevskii, *Electrodynamics of Continuous Media* (Butterworth-Heinemann, London, 1995), p. 212.
- ⁸A. Yelon, D. Ménard, M. Britel, and P. Cireanu, *Appl. Phys. Lett.* **69**, 3084 (1996).
- ⁹L. Kraus, *J. Magn. Magn. Mater.* **195**, 764 (1999).
- ¹⁰F. L. A. Machado and S. M. Rezende, *J. Appl. Phys.* **79**, 6558 (1996).
- ¹¹D.-X. Chen, J. L. Muñoz, A. Hernando, and M. Vázquez, *Phys. Rev. B* **57**, 10699 (1998).
- ¹²L. V. Panina, K. Mohri, T. Uchiyama, M. Noda, and K. Bushida, *IEEE Trans. Magn.* **30**, 1249 (1995).
- ¹³A. Atkinson and P. T. Squire, *J. Appl. Phys.* **83**, 6569 (1998).
- ¹⁴L. Kraus, M. Knobel, S. N. Kane, and H. Chiriach, *J. Appl. Phys.* **85**, 5435 (1999).
- ¹⁵C. G. Kim, K. J. Janh, D. Y. Kim, and S. S. Yon, *Appl. Phys. Lett.* **75**, 2114 (1999).
- ¹⁶C. Gómez-Polo and M. Vázquez, *J. Magn. Magn. Mater.* **118**, 86 (1993).
- ¹⁷L. V. Panina, K. Mohri, and D. P. Makhnovskiy, *J. Appl. Phys.* **85**, 5444 (1999).
- ¹⁸D.-X. Chen, L. Pascual, and A. Hernando, *Appl. Phys. Lett.* **77**, 1727 (2000).
- ¹⁹C. G. Kim, K. J. Jang, D. Y. Kim, and S. S. Yoon, *Appl. Phys. Lett.* **77**, 1730 (2000).